DOI: 10.1002/asia.200800362

Magneto-Structural Correlations in a 1,3,2-Dithiazolyl Radical Crystal, BBDTA·$GaBr_4$: Structure and Magnetic Properties of its Three Polymorphs

Wataru Fujita* and Koichi Kikuchi[a]

Dedicated to the late Professor Kazuhiko Seki

Abstract: We investigate the preparation, crystal growth, crystal structure, and magnetic properties of the three polymorphs (α, β, and γ) of an organic magnet, BBDTA(=benzo[1,2-d:4,5-d′] bis[1,3,2]dithiazole)·$GaBr_4$, which is an *S*-1/2 system. In the α phase, $BBDTA^+$ units form a square-planar lattice, and show canted antiferromagnetism with a magnetic coupling constant J/k_B of −18 K and a canting angle of 0.15° below 15.5 K. The β phase is composed of a ferromagnetic regular chain with a J/k_B value of +4.5 K and a strong antiferromagnetic chain with $J/k_B = -99$ K, and shows ferromagnetic ordering in spins of purely the ferromagnetic chain below 0.4 K. The γ phase is isostructural with γ-BBDTA·$GaCl_4$, which is an organic ferromagnet below 7.0 K, and possesses antiferromagnetic interactions of $J/k_B = -60$ K between $BBDTA^+$ cations, and shows no magnetic ordering until 2 K. The magnetic properties of these phases are quite sensitive to the molecular alignment in the crystals.

Keywords: crystal growth · magnetic properties · molecule-based magnets · phase transitions · radicals

Introduction

Cyclic thiazyl radicals exhibit strong intermolecular interactions by the characteristic S···N and/or S···S contacts between the molecules and easily form multi-dimensional networks in their solid state.[1] Such properties as magnetic ordering,[2] room-temperature magnetic bistability,[3] photoinduced phase transition,[4] metallic conduction,[5] and negative resistance[6] have been identified in these materials, which makes them highly attractive as building blocks of molecule-based magnetic materials.[7] Recently, Oakley and co-workers found ferromagnetic ordering at 12.3 K and 17 K, and weak ferromagnetism below 18 K and 27 K in *bis*-selena/thiazolyl radicals.[8] These transition temperatures are very much higher than those typically observed for other organic-radical-based magnetic materials.

We focus on the monocationic dithiazolyl radical ($S = 1/2$) of benzo[1,2-d:4,5-d′]bis[1,3,2]dithiazole (BBDTA), whose molecular structure is presented in Scheme 1. Wolmershäuser et al. were the first to report the crystal structure and ^{57}Fe Mössbauer spectra of the radical cation salt BBDTA·$FeCl_4$·CH_3CN.[9] In this material, $BBDTA^+$ formed a face-to-face dimer structure, accompanied by two solvent molecules of CH_3CN, and antiferromagnetic ordering was observed for only the $FeCl_4^-$ magnetic moments below 6.6 K. We have systematically investigated the crystal structure and magnetic properties of BBDTA cation radical salts with various counter anions in search of new magnetic materials with a higher magnetic transition temperature. Recently, we have found ferromagnetic ordering in the salts γ-BBDTA·$GaCl_4$ and BBDTA·$FeCl_4$ below 7.0 K and 44.5 K, respectively.[10] In InX_4 (X = Cl, Br) derivatives, a one-dimensional coordination polymer structure was formed, and the spin Peierls transition occurred at 108 K and 250 K, respectively.[11] Thus, these cationic salts show various crystal structures and magnetic phase transitions at relatively higher temperatures.

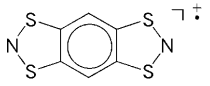

Scheme 1. $BBDTA^+$ radical cation.

[a] Prof. Dr. W. Fujita, Prof. Dr. K. Kikuchi
Department of Chemistry
Tokyo Metropolitan University
Minami-osawa 1-1, Hashioji 192-0397 (Japan)
Fax: (+81) 42-677-2525
E-mail: fujitaw@tmu.ac.jp

In the present study, we focus on the gallium bromide derivative BBDTAGaBr$_4$. This salt has three polymorphs: α, β, and γ. Although we have briefly reported the ferromagnetic phase transition of the β phase in the ultralow temperature region, herein we describe in detail the preparation, isolation, crystal structure, and magnetic properties of the three polymorphs of this salt.

Results and Discussion

Crystal Structure

We obtained three polymorphs of BBDTA·GaBr$_4$ (α, β, and γ) by slow cooling or layering methods from the appropriate solutions. The structures of the resulting crystals were determined by using X-ray crystallographic analysis. The details are described in the Experimental Section. The crystallographic data are summarized in Table 1.

Table 1. Crystallographic data for the three polymorphs of BBDTA·GaBr$_4$.

	α	β	γ
Crystal system	orthorhombic	monoclinic	monoclinic
Space group	*Pnma*	$P2_1/c$	$C2/c$
a [Å]	10.000(6)	8.075(4)	11.680(6)
b [Å]	16.528(9)	13.865(7)	10.944(8)
c [Å]	9.087(5)	13.612(7)	13.474(7)
β [°]	90	95.596(2)	114.076(4)
V [Å^3]	1501.90(15)	1516.73(13)	1572.5(2)
Z	4	4	4
R_1	0.0445	0.0638	0.0510
wR_2	0.1056	0.1429	0.1149

The α phase: Figure 1 shows the crystal structure of the α phase, which is assigned to an orthorhombic *Pnma* space group with half of the molecule crystallographically asymmetric. This crystal is comprised of a stack of alternating BBDTA$^+$ cation-assembled layers and GaBr$_4$ anion layers, as shown in Figure 1a. Figure 1b depicts the molecular alignment of BBDTA$^+$ in the layer. BBDTA$^+$ did not form a dimer or π-stacking columnar structure, but a square-planar lattice by the intermolecular S···C interatomic contacts of 3.411 (6) Å and 3.417 (6) Å, shown as broken lines. Figure 1c presents a space-filling model of the cation layer. The marked sphere corresponds to bromide atoms of the GaBr$_4^-$ counter anion. Each bromide atom was surrounded by four BBDTA$^+$ cations. It seems that the molecular alignment in the organic radical layer may not be governed by the intermolecular interatomic S···S or S···N contacts, which are characteristic of the cyclic thiazyl radicals, but the Coulombic interaction between the anion and cation.

The β phase: Figure 2 shows the crystal structure of the β phase, which is assigned to a monoclinic $P2_1/c$ space group with two BBDTA$^+$ cations crystallographically asymmetric. In this crystal, BBDTA$^+$ cations form a sheet in the *ab* plane as shown in Figure 2a, and the sheets are laminated along the *c* axis. Counter anions are positioned between the

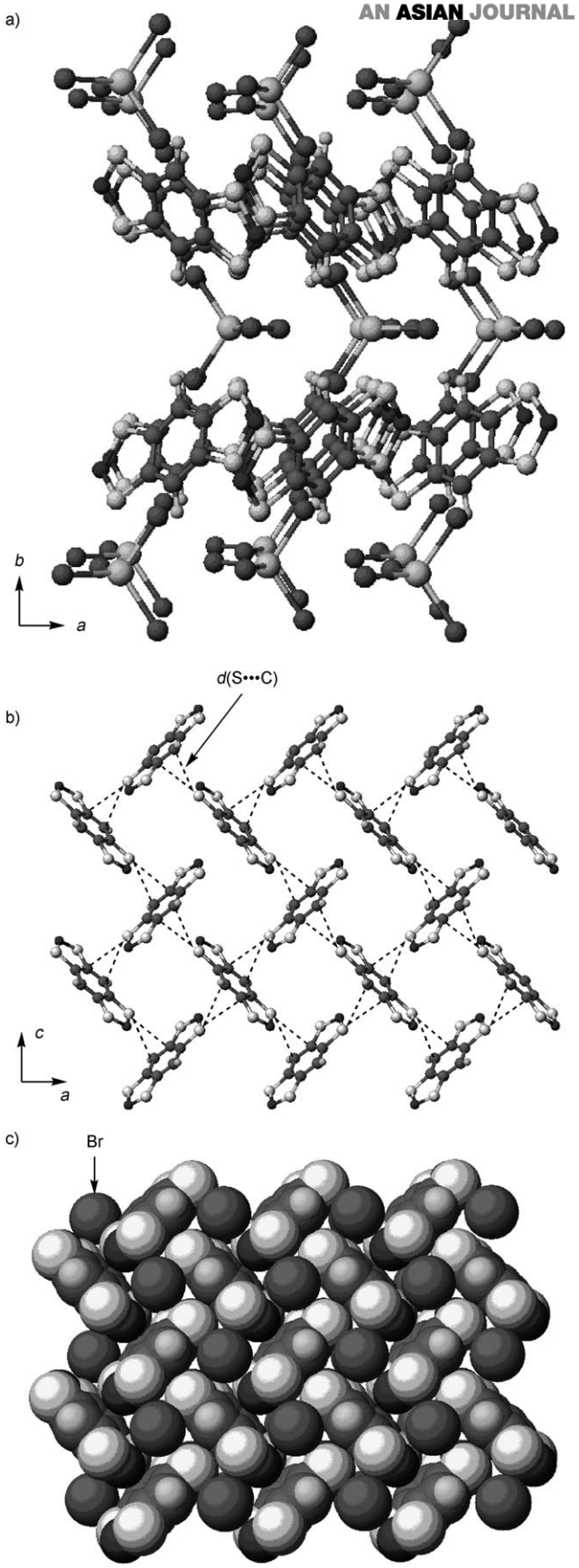

Figure 1. Crystal structure of α-BBDTA·GaBr$_4$: a) layered structure composed of BBDTA$^+$ and counter anion, b) molecular alignment of the organic radical layer, c) a space-filling model of the organic layer and Br atoms of the counter anion.

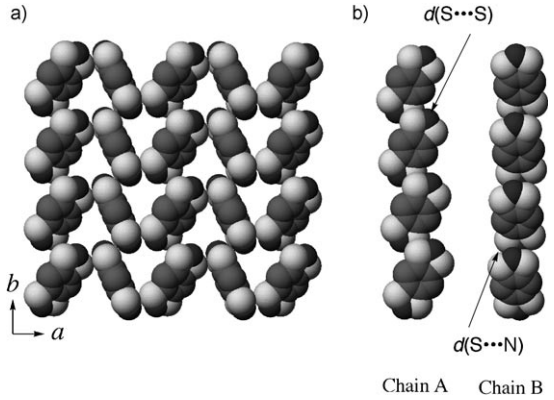

Figure 2. Crystal structure of b-BBDTA·$GaBr_4$: a) molecular alignment of the organic radical layer in the *ab* plane, b) two types of the molecular chain, A and B.

sheets. There are two kinds of one-dimensional alignment of $BBDTA^+$ cations in the sheet, which consists of an alternating alignment of chains. Figure 2b shows the molecular alignment of $BBDTA^+$ cations in the two chains, labelled Chain A and Chain B. In Chain A, the closest intermolecular contact was S···S at 3.732 (4) Å, whereas in chain B, it was S···N at 3.393 (10) Å, as marked by arrows. The β phase is expected to exhibit a two-dimensional magnetic behavior or a magnetic behavior arising from two kinds of one-dimensional networks.

The γ phase: Figure 3 shows the crystal structure of the γ phase, which is isostructural to that of the organic ferromagnet γ-BBDTA·$GaCl_4$. The nearest neighboring $BBDTA^+$

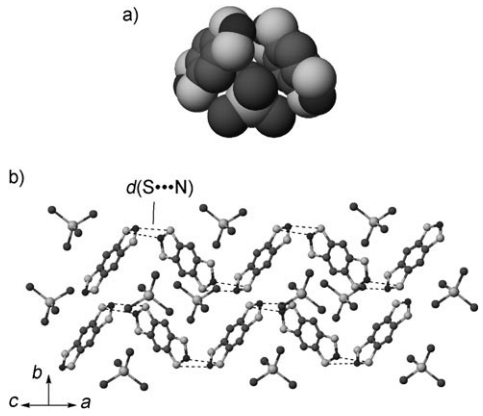

Figure 3. Crystal structure of γ-BBDTA·$GaBr_4$: a) nearest-neighbor intermolecular arrangement, b) molecular alignment onto the (1 1 −1) plane.

cations sandwiched a tetrahedron of $GaBr_4^-$, as shown in Figure 3a. There are two short intermolecular S···N contacts of 3.332(2) Å in the pair (broken lines), whereby the BBDTA forms a one-dimensional (1D) zigzag network along the *c*-axis (Figure 3b). There is no short interatomic contact in the interchain arrangement. It is predicted that the γ phase has a 1D magnetic network.

Magnetic Properties

The α phase: Figure 4 plots the temperature dependence of paramagnetic susceptibility under 5 kOe and the field dependence of magnetization at 2 K for the α phase. As shown

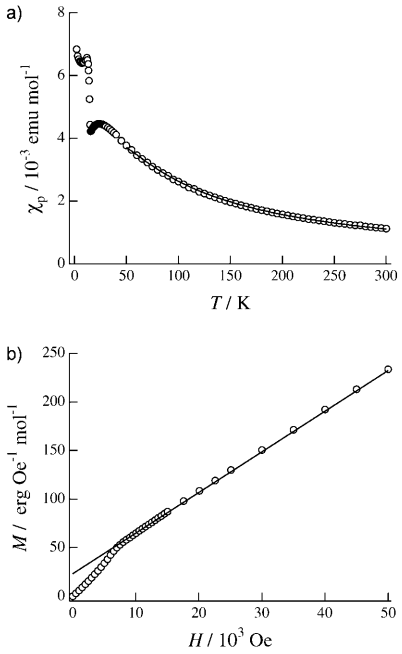

Figure 4. Magnetic data for α-BBDTA·$GaBr_4$: a) temperature dependence of χ_p, b) magnetization curve at 2 K.

in Figure 4a, the χ_pT value at 300 K was 0.251 emu K mol^{-1}, which is less than the predicted value of 0.375 emu K mol^{-1} in the case of no magnetic interaction between the unpaired electrons of $g=2$ and $S=1/2$.[13] This indicates the predominance of an antiferromagnetic interaction between neighboring $BBDTA^+$ cations in the organic layer. A plot of the molar susceptibility versus temperature exhibited a broad maximum at 24 K, presumably arising from a short-range magnetic order associated with the two-dimensional structural character. At 15.5 K, the susceptibility increased rather sharply. This behavior is characteristic of antiferromagnetic phase transitions with slight spin canting. Canted antiferromagnetism has been observed in certain organic-based magnetic materials.[14] We can regard the α phase as a two-dimensional magnetic system because the diamagnetic $GaBr_4$-anion layers separate the organic-radical layers. The paramagnetic susceptibility above 50 K could be reproduced by the theoretical equation for the two-dimensional square-lattice model,[15]

$$\chi_p = \frac{C}{T}[1 + \sum_{n\geq 1}(\alpha_n/2^n n!)z^n] \quad (1),$$

in which C is the Curie constant, $z=J/k_BT$, J is the intermolecular exchange coupling constant, and the coefficients an

are as follows: $a_1=4$, $a_2=16$, $a_3=64$, $a_4=416$, $a_5=4544$, $a_6=23488$, $a_7=-207616$, $a_8=4205056$, $a_9=198295552$, and $a_{10}=-2574439424$. The magnetic parameters $C=0.375$ emu K mol^{-1}(fixed) and $J/k_B=-18$ K were estimated by curve fitting, as shown by the solid curve in Figure 4a. Figure 4b depicts the field dependence of magnetization of the α phase at 2 K. Magnetization of this phase gradually increased with increasing magnetic field. This is typical for an antiferromagnet. An anomaly was observed near 7500 Oe. We interpret this field dependence as follows: spin canting in this phase may induce a large magnetic moment in the organic layer and the weak antiparallel coupling between the organic layers cancel the magnetic moments. It seems that the antiparallel alignment of the magnetic moments between the organic layers is broken up at an external magnetic field of about 7500 Oe. The magnetization arising from spin canting in the organic layer was 22.5 erg Oe^{-1} mol^{-1}, as estimated by extrapolating the magnetization above 10 kOe. The canting angle from the antiparallel alignment of spins was approximately 0.12°, which was consistent with those of other organic weak ferromagnets. Thus, the α phase showed canted antiferromagnetic behavior below 15.5 K. This Néel temperature was relatively high, compared to those of traditional aminoxyl-based antiferromagnets.[16]

The β phase: Figure 5 plots the temperature dependence of paramagnetic susceptibility under 5 kOe and the field dependence of magnetization at 2 K for the β phase. Figure 5a shows the χ_pT versus T plot. There were two distinct temperature dependences. The χ_pT value was 0.289 emu K mol^{-1} at 300 K and decreased with decreasing temperature down to 40 K, suggesting the dominance of antiferromagnetic intermolecular interactions. The χ_pT value increased with decreasing temperature below 40 K, reaching 0.483 emu K mol^{-1} at 2 K. This suggests that there is a ferromagnetic intermolecular interaction in the β phase. No magnetic phase transition was observed in the β phase in the 2–300 K range. Figure 5b plots the field dependence of magnetization for the β phase at 2 K. The magnetization increased rapidly, as in a typical ferromagnet, and saturated above around 30 kOe. The magnetization was 2789 erg Oe^{-1} mol^{-1} at 50 kOe, which is almost half the theoretical saturation (5585 erg Oe^{-1} mol^{-1}) for ferromagnetic species with $S=1/2$ and $g=2$.[15] We have already reported the magnetic and thermal properties of the β phase below 1 K.[12] We have found that only half of the unpaired electrons in the sample showed ferromagnetic ordering below 0.4 K. We can easily expect that the β phase was an immiscible combination of the ferromagnetic and antiferromagnetic components. The crystal structure of the β phase led us to the conclusion that its magnetic behavior is a result of the two magnetic chains, one with a strong antiferromagnetic interaction, J_{AF}, and the other with a weak ferromagnetic interaction J_F. The magnetic parameters of the β phase were estimated using the following theoretical model, which incorporates the one-dimensional ferromagnetic Heisenberg model and the Bonner–Fisher model,[17,18]

$$\chi_pT = 0.5C\,[(1.0+0.5998y+1.20376y^2)/(1+1.9862y+0.68854y^2+6.0626y^3)+\{(1.0+5.79799\,K+16.902653\,K^2+29.376885\,K^3+29.832959\,K^4+14.036918\,K^5)/(1.0+2.7979916\,K+7.0086780\,K^2+8.6538644\,K^3+4.5743114\,K^4)\}^{2/3}] \quad (2),$$

in which $y=|J_{AF}|/k_BT$ and $K=J_F/2k_BT$. The solid curve in Figure 5 is the best fit with the parameters $C=0.375$ emu K mol^{-1}(fixed), $J_{AF}/k_B=-99$ K, and $J_F/k_B=+4.5$ K. The measured magnetic data were well-reproduced by the theoretical curve. This indicates that the magnetic properties of the β phase reflect two independent magnetic chains, one with a strong antiferromagnetic interaction and the other, a weak ferromagnetic interaction above 2 K.

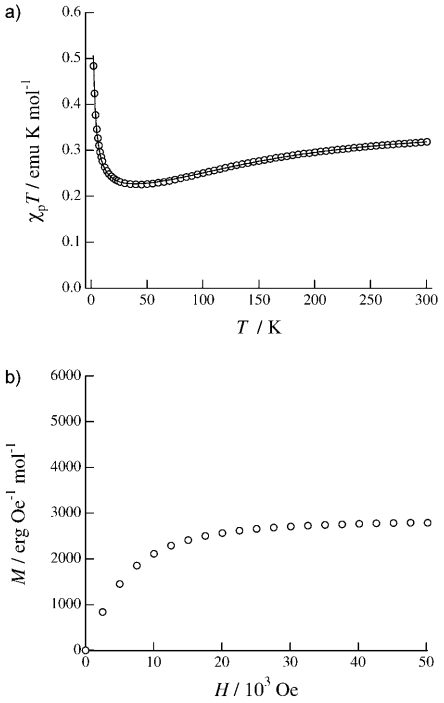

Figure 5. Magnetic data for β-BBDTA·GaBr$_4$: a) temperature dependence of χ_pT, b) magnetization curve at 2 K.

The γ phase: Figure 6 plots the temperature dependence of χ_pT for the γ phase under 5 kOe. The χ_pT value decreased with decreasing temperature in this case as well, suggesting the dominance of antiferromagnetic intermolecular interactions. There was no magnetic phase transition in the temperature range 2–300 K. We estimated the magnetic parameters by using the Bonner–Fisher equation with the Curie term arising from magnetic impurities and lattice defects,

$$\chi_pT = 4\,(C-C_{imp})\cdot(0.25+0.14995y+0.30094y^2)/(1+1.9862y+0.68854y^2+6.0626y^3)+C_{imp} \quad (3),$$

in which C_{imp} is the Curie constant of magnetic impurities and/or lattice defects, which behave as Curie paramagnets. The magnetic data could be reproduced by the above model

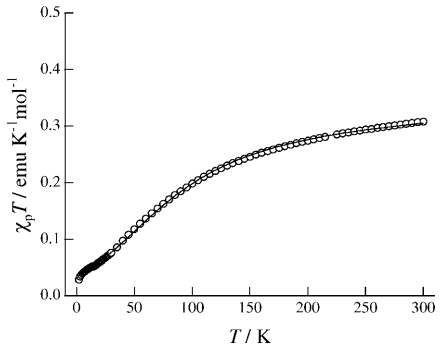

Figure 6. Temperature dependence of $\chi_p T$ for γ-BBDTA·$GaBr_4$.

using the parameters $C = 0.375$ emu K mol^{-1} (fixed), $C_{imp} = 0.0335$ emu K mol^{-1}, and $J/k_B = -60$ K.

The organic ferromagnet γ-BBDTA·$GaCl_4$ was isostructural with the γ phase of BBDTA·$GaBr_4$, and showed a ferromagnetic phase transition at 7.0 K,[10a] in contrast to the antiferromagnetic behavior of the γ phase. In general, intermolecular magnetic interactions in organic radical crystals are governed by the nearest-neighbor overlaps between the magnetic orbitals.[19] An orthogonal relation between neighboring singly occupied molecular orbitals (SOMO) induces a ferromagnetic interaction, whereas an overlap between them produces an antiferromagnetic interaction. Although the γ phase of BBDTA·$GaBr_4$ is isostructural with γ-BBDTA·$GaCl_4$, the molecular configuration of the neighboring $BBDTA^+$ cations in the two materials may be different. Figure 7 shows the SOMO of the BBDTA radical cation and molecular alignments, and their schematic representations of intermolecular interatomic S···N contacts in both phases. The SOMO has an extended population on the molecular plane and a characteristic nodal plane in each S–N bond, as shown in Figure 7a. Figure 7b shows the nearest-neighbor molecular contact in the ferromagnetic derivative γ-BBDTA·$GaCl_4$, corresponding to the top view of a molecular configuration as in Figure 3a. The nitrogen atom in the lower molecule is close to the center of the SN bond in the upper molecule in γ-BBDTA·$GaCl_4$. Thus, the overlap integral in the region in which the product of these SOMOs is positive, cancels that in the region in which the product is negative, as shown in Figure 7d. In γ-BBDTA·$GaCl_4$, the minimal overlap between the SOMOs is likely to cause a ferromagnetic coupling between the molecules. Figure 7c depicts the nearest-neighbor contact in the antiferromagnetic derivative, γ-BBDTA·$GaBr_4$. The nitrogen atom in the lower molecule is located slightly to the left of the center of the SN bond in the other molecule. As a result, there may be a net overlap between the SOMOs because the positive overlap does not cancel the negative overlap. It is thought that this is the cause of the antiferromagnetic properties observed in the γ phase of BBDTA·$GaBr_4$. This illustrates again that the magnetic properties of molecule-based magnetic materials are very sensitive to the crystal structure. Thus, the γ phase was a one-dimensional paramagnet with intermolecular antiferromagnetic interactions. It is interesting that a small difference in the molecular alignment should lead to such a dramatic difference in magnetic properties.

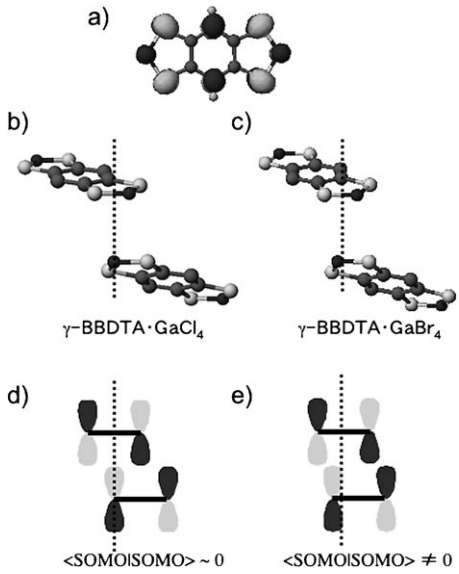

Figure 7. a) SOMO of $BBDTA^+$, overlap of the SOMOs in the nearest-neighbor molecular arrangement in b) γ-BBDTA·$GaCl_4$ and c) γ-BBDTA·$GaBr_4$, schematic of the relative configuration of the SOMOs in the nearest orientation in d) γ-BBDTA·$GaCl_4$ and e) γ-BBDTA·$GaBr_4$.

Conclusions

In this paper, we report the preparation, isolation, structure, and magnetic properties of three polymorphs (α, β, and γ) of the cation radical salt BBDTA·$GaBr_4$. In the α phase, $BBDTA^+$ cations form a square-planar lattice alignment, and show canted antiferromagnetism below 15.5 K. The β phase is composed of a weak ferromagnetic regular chain and a strong antiferromagnetic chain, and shows ferromagnetic ordering in spins of purely the ferromagnetic chains below 0.4 K. The γ phase is isostructural with an organic ferromagnet below 7.0 K, γ-BBDTA·$GaCl_4$, exhibits antiferromagnetic interactions between $BBDTA^+$ cations, but shows no magnetic ordering up to 2 K. Thus, various magnetic networks are formed in the three polymorphs of this cation radical salt. Magnetic properties of the cationic salts are very sensitive to the relative configuration of neighboring molecules in the crystals, such as γ-BBDTA·$GaCl_4$ and γ-BBDTA·$GaBr_4$. Finally, chemical modification of cyclic thiazyl radical ions and their combination with appropriate counter anions may lead to novel magnetic networks of interest to solid state physicists or high-T_C molecule-based ferromagnets that many chemists wish to synthesize.

Experimental Section

$BBDTA{\cdot}GaBr_4$ was synthesized as follows: $BBDTA{\cdot}FeCl_4{\cdot}CH_3CN$[9,20] was mixed with excess tetra(*n*-butylammonium) bromide in CH_3CN. The brown BBDTA·Br precipitate obtained was dried under vacuum, and then reacted with $GaBr_3$ for 2 h in acetonitorile under nitrogen atmosphere. The solution immediately turned deep green. A greenish $BBDTA{\cdot}GaBr_4$ powder was obtained upon evaporation of the solvent. We found at least three polymorphs of $BBDTA{\cdot}GaBr_4$, namely, α (dark-greenish needles), β (dark-greenish blocks), and γ (dark-greenish cuboids). The α phase often crystallized from a 1:1 mixed solvent of acetone and dichloromethane at −23°C. The β phase was prepared by recrystallization from a 1:1 mixed solvent of nitromethane and dichloromethane at −23°C. The γ phase was obtained as a mixture with the α and β phases by layering an acetone solution of the salt with diethyl ether. Then the two phases were separated from the sample of the γ phase under a microscope as soon as possible.

X-ray diffraction data were collected with a graphite-monochromated $Mo{-}K_\alpha$ ($\lambda = 0.71073$ Å) radiation on a Mac Science DIP-3200 imaging plate diffractometer. All structures were solved by a direct method using the SHELXS-97 program[21] and refined by successive differential Fourier syntheses and a full-matrix least-squares procedure using the SHELXL-97 program.[22] Anisotropic thermal factors were applied to all non-hydrogen atoms.

CCDC 698637 (the α phase), CCDC 698638 (the β phase), CCDC 698639 (the γ phase) contain the supplementary crystallographic data for this paper. These data can be obtained free of charge from The Cambridge Crystallographic Data Centre at www.ccdc.cam.ac.uk/data_request/cif

Magnetic measurements were carried out on a SQUID (Quantum Design MPMS XL) magnetometer under 5000 Oe. The experimental raw data were corrected for diamagnetism and the molar paramagnetic susceptibilities were obtained.

Acknowledgements

This work was partially supported by the Tokuyama Science Foundation and by a Grant-in-Aid for Scientific Research (No. 19550139) from the Ministry of Education, Culture, Sports, Science and Technology of Japan. We thank Hirokazu Sakamoto for his kind help in magnetic measurements.

[1] K. Awaga, T. Tanaka, T. Shirai, M. Fujimori, Y. Suzuki, H. Yoshikawa, W. Fujita, *Bull. Chem. Soc. Jpn.* **2006**, *79*, 25–34.

[2] a) A. J. Banister, N. Bricklebank, I. Lavender, J. M. Rawson, C. I. Gregory, B. K. Tanner, W. Clegg, M. R. J. Elsegood, F. Palacio, *Angew. Chem.* **1996**, *108*, 2648–2650; *Angew. Chem. Int. Ed. Engl.* **1996**, *35*, 2533–2535; b) A. Alberola, R. J. Less, C. M. Pask, J. M. Rawson, F. Palacio, P. Oliete, C. Paulsen, A. Yamaguchi, R. D. Farley, D. M. Murphy, *Angew. Chem. Int. Ed.* **2003**, *42*, 4782–4785.

[3] a) W. Fujita, K. Awaga, *Science* **1999**, *286*, 261–262; b) W. Fujita, K. Awaga, H. Matsuzaki, H. Okamoto, *Phys. Rev. B* **2002**, *65*, 064434.

[4] H. Matsuzaki, W. Fujita, K. Awaga, H. Okamoto, *Phys. Rev. Lett.* **2003**, *91*, 017403.

[5] C. D. Bryan, A. W. Cordes, R. M. Fleming, N. A. George, S. H. Glarum, R. C. Haddon, R. T. Oakley, T. T. M. Palstra, A. S. Perel, L. F. Schneemeyer, J. V. Waszczak, *Nature* **1993**, *365*, 821–823.

[6] a) K. Okamoto, T. Tanaka, W. Fujita, K. Awaga, T. Inabe, *Angew. Chem.* **2006**, *118*, 4628–4630; *Angew. Chem. Int. Ed.* **2006**, *45*, 4516–4518; b) K. Okamoto, T. Tanaka, W. Fujita, K. Awaga, *Phys. Rev. B* **2007**, *76*, 075328.

[7] a) J. M. Rawson, F. Palacio, *Struct. Bonding* **2001**, *100*, 93–128; b) K. E. Preuss, *Dalton Trans.* **2007**, 2357–2369; c) J. M. Rawson, A. Alberola, A. Whalley, *J. Mater. Chem.* **2006**, *16*, 2560–2575.

[8] a) A. A. Leitch, J. L. Brusso, K. Cvrkalj, R. W. Reed, C. M. Robertson, P. A. Dube, R. T. Oakley, *Chem. Commun.* **2007**, 3368–3371; b) C. M. Robertson, D. J. T. Myles, A. A. Leitch, R. W. Reed, B. M. Dooley, N. L. Frank, P. A. Dube, L .K. Thompson, R. T. Oakley, *J. Am. Chem. Soc.* **2007**, *129*, 12688–12689; c) C. M. Robertson, A. A. Leitch, K. Cvrkalj, R. W. Reed, D. J. T. Myles, P. A. Dube, R. T. Oakley, *J. Am. Chem. Soc.* **2008**, *130*, 8414–8425.

[9] G. Wolmershäuser, G. Wortman, M. Schnauber, *J. Chem. Res. Synop.* **1988**, 358–359.

[10] a) W. Fujita, K. Awaga, *Chem. Phys. Lett.* **2004**, *388*, 186–189; b) W. Fujita, K. Awaga, M. Takahashi, M. Takeda, T. Yamazaki, *Chem. Phys. Lett.* **2002**, *362*, 97–102.

[11] a) W. Fujita, K. Awaga, R. Kondo, S. Kagoshima, *J. Am. Chem. Soc.* **2006**, *128*, 6016–6017; b) W. Fujita, K. Kikuchi, K. Awaga, *Angew. Chem.* **2008**, *120*, 9622–9625; *Angew. Chem. Int. Ed.* **2008**, *47*, 9480–9483.

[12] K. Shimizu, T. Gotohda, T. Matsushita, N. Wada, W. Fujita, K. Awaga, Y. Saiga, D. S. Hirashima, *Phys. Rev. A* **2006**, *74*, 013801.

[13] L. R. Carlin, *Magnetochemistry*, Springer, Heidelberg, **1986**.

[14] a) S. Tomiyoshi, T. Yano, N. Azuma, M. Shoga, K. Yamada, J. Yamauchi, *Phys. Rev. B* **1994**, *49*, 16031; b) T. Sugimoto, M. Tsuji, H. Matsuura, N. Hosoito, *Chem. Phys. Lett.* **1995**, *235*, 183–186; c) M. Mito, H. Nakano, T. Kawase, M. Hitaka, S. Takagi, H. Deguchi, K. Suzuki, K. Mukai, K. Takeda, *J. Phys. Soc. Jpn.* **1997**, *66*, 2147–2156; d) H. Akutsu, K. Saito, M. Sorai, *Phys. Rev. B* **2000**, *61*, 4346/1–7.

[15] G. A. Baker, H. E. Gilbert, J. Eve, G. S. Rushbrooke, *Phys. Rev.* **1967**, *164*, 800–817.

[16] a) Y. Nakazawa, M. Tamura, N. Shirakawa, D. Shiomi, M. Takahashi, M. Kinoshita, M. Ishikawa, *Phys. Rev. B* **1992**, *46*, 8906–8914; b) K. Togashi, R. Imachi, K. Tomioka, H. Tsuboi, T. Ishida, T. Nogami, N. Takeda, M. Ishikawa, *Bull. Chem. Soc. Jpn.* **1996**, *69*, 2821–2830.

[17] a) J. C. Bonner, M. E. Fisher, *Phys. Rev.* **1964**, *135*, A640–658; b) W. E. Hatfield, *J. Appl. Phys.* **1981**, *52*, 1985–1990.

[18] G. A. Baker, Jr., G. S. Rushbrooke, H. E. Gilbert, *Phys. Rev.* **1964**, *135*, A1272–A1277.

[19] *Magnetic Properties of Organic Materials* (Ed.: P. M. Lahti), Marcel Dekker, New York, **1999**.

[20] a) E. Dormann, M. J. Nowak, K. A. Williams, R. O. Angus, F. Wudl, *J. Am. Chem. Soc.* **1987**, *109*, 2594–2599; b) T. M. Barclay, A. W. Cordes, R. H. de Laat, J. D. Goddard, R. C. Haddon, D. Y. Jeter, R. C. Mawhinney, R. T. Oakley, T. T. M. Palstra, G. W. Patenaude, R. W. Reed, N. P. C. Westwood, *J. Am. Chem. Soc.* **1997**, *119*, 2633–2641.

[21] G. M. Sheldrick SHELXS-97: Program for crystal structure solution, University of Gottingen (Germany), **1997**.

[22] G. M. Sheldrick SHELXL-97: Program for crystal structure solution, University of Gottingen (Germany), **1997**.

Received: September 17, 2008
Published online: December 8, 2008

